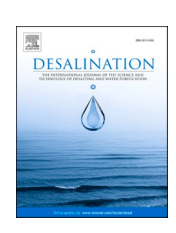


Contents lists available at ScienceDirect

# Desalination

journal homepage: www.elsevier.com/locate/desal





# Root cause analysis for membrane system validation failure at a full-scale recycled water treatment plant

Marlene Cran<sup>a</sup>, Stephen Gray<sup>a</sup>, Jonathan Schmidt<sup>b</sup>, Li Gao<sup>a,b,\*</sup>

- <sup>a</sup> Institute for Sustainable Industries and Liveable Cities. Victoria University. PO Box 14428. Melbourne. Victoria 8001. Australia
- <sup>b</sup> South East Water, 101 Wells Street, Frankston, Victoria 3199, Australia

#### HIGHLIGHTS

- Root cause analysis for membrane system validation failure
- Chemical oxidation resulted in membrane structure change
- Inappropriate chemical enhanced backwash led to rapid membrane degradation.
- Site investigation and field testing for full scale membrane plant

#### ARTICLE INFO

#### Keywords: Root cause analysis Membrane validation Challenge test LRV Pathogen removal

#### ABSTRACT

Ultrafiltration (UF) membranes can be used as a standalone process for the removal of enteric virus and are often combined with reverse osmosis (RO) processes for use as the pre-treatment to manage microbial risks. In this study, a water utility experienced multiple validation failures in one of its UF plants with virus log reduction values (LRV) as low as 0.79 reported. This resulted in the suspension of recycled water supply to customers and initiated a comprehensive root cause analysis to identify the reason for the unusually rapid membrane degradation and virus removal validation failure. Polyethersulfone (PES) membrane fibres were sampled from the used modules and a systematic autopsy was undertaken. The FTIR spectroscopic structural analysis revealed oxidative changes in the PES polymer structure. Thermal analysis by differential scanning calorimetry showed changes in the melting point of the PES and suggested a loss of the pore-forming polymer polyvinylpyrrolidone (PVP). Streaming potential analysis showed a decrease in the negativity of the surface charge from -50~mV to -30~mVat pH 7. Tensile testing revealed a 9% and 47% decrease in the breaking force and elongation at break of the used fibres respectively. The pore size evaluation challenge testing of the used fibres showed no rejection of nanoparticles with 150 nm diameter and smaller. The autopsy investigation suggested that the unusually rapid membrane degradation was due to chemical oxidation resulting in changes in the PES structure and physical properties. Detailed on-site investigation was then undertaken and it was suggested that the failure to operate appropriate chemical enhance backwash (CEB) was the main cause for the unusually rapid virus LRV reduction. Finally, CEB water sampling and analysis were undertaken, which confirmed the recommendations from membrane autopsy and site investigation. A range of system improvements (system control, new inline static mixer, CEB water quality monitoring, etc.) were implemented. Based on the root cause analysis and system improvements, the maximum virus LRV of 4 has been maintained since then.

#### 1. Introduction

Water scarcity has become a global concern due to the combined effects of climate change, population growth and water quality deterioration [1]. Although novel treatment technologies have been

developed, such as UV-LED [2,3], photo catalytic oxidation [4,5], and algae-based water treatment [6–8], they are at the early stage of implementation. Membrane technology still plays an essential role in supplying high quality water for different purposes [9,10]. One of the main advantages for membrane technology is its high treatment

<sup>\*</sup> Corresponding author at: Institute for Sustainable Industries and Liveable Cities, Victoria University, PO Box 14428, Melbourne, Victoria 8001, Australia. E-mail address: li.gao@sew.com.au (L. Gao).

performance for pathogen removal, including virus, bacteria and protozoa [11]. The size of enteric virus is between 20 and 160 nm [12], which is generally smaller than bacteria and protozoa [13], therefore, virus removal efficiency is used as an indicator to ensure the treatment performance of membrane systems based on size exclusion. The most common membrane technologies employed for water purification include high-pressure membranes (nanofiltration (NF) and reverse osmosis (RO)), and low-pressure membranes (ultrafiltration (UF) and microfiltration (MF)), and the main characteristics of these systems is presented in Table 1.

It is generally accepted that a multi-barrier approach should be applied to manage water quality risks, especially for microbial contaminants, because public health protection should not only rely on a single treatment process. Based on this consideration, UF is often combined with RO process and used as the pre-treatment to manage the microbial water quality risks. In addition, algae blooms can occur under different environmental conditions [20,21], which can cause serious operational issues for RO membranes. UF can also effectively remove algae and other physical contaminants from the raw water [22]. Wolf et al. [22] have analyzed different pre-treatment systems for RO process and suggested that UF is the most preferred choice, as it provides an effective barrier to not only particulates but also pathogens, and ensures a consistent and desired feed water quality to the RO system. Hong et al. [23] also investigated the treatment performance of an integrated UF-RO desalination plant located at the Arabian Gulf. Their results showed that a large portion of the microbial communities (60.5%) in the UF feedwater were removed by UF pre-treatment.

Although an integrated UF-RO system can provide effective removal of enteric virus, membrane integrity can be compromised and its performance degraded over time due to various reasons, including membrane material degradation, membrane fouling and scaling or mechanical/membrane surface damage. To actively monitor membrane integrity and its treatment performance, different methods can be utilized. Filtrate quality monitoring is one of the most widely used approaches to measure membrane integrity, and the monitored water quality parameters include turbidity for MF and UF, and conductivity and total organic carbon for RO. Pressure decay and vacuum decay tests are also often utilized as part of the daily operational program to verify the membrane integrity of low-pressure membranes. However, the above methods are considered as indirect approaches, and correlations have to be established between the measured parameters and the membrane virus removal performance with conservative estimates of log removal value (LRV) credited to the systems [19].

To satisfy the sensitivity, accuracy and resolution requirements of monitoring, a direct integrity test is required to verify the membrane condition and ensure high virus removal efficiency. Challenge testing with MS2 bacteriophage is currently the most popular validation method, which is relatively simple to perform although the tested membrane skid must be offline during the test. During the challenge test, a high concentration of MS2 bacteriophage is dosed into the membrane feed, the corresponding filtrate is then sampled and the residual MS2 bacteriophage concentration in the filtrate is analyzed. The validation result is quantified by the LRV, which is calculated based on the logarithm of the ratio of pathogen concentration in the influent and effluent of the membrane process (Eq. (1)) [24].

**Table 1**Characteristics of membrane processes.

Membrane	Pore size	Virus removal characteristics	
MF UF NF/RO	>0.1 µm 10–100 nm <10 nm [11,18]	Low virus removal [14,15] High enteric virus removal [16,17] High virus removal, cake layer/fouling can improve virus removal [19]	

$$LRV = log_{10} \left( \frac{C_{in}}{C_{eff}} \right) \tag{1}$$

Here,  $C_{\rm in}$  and  $C_{\rm eff}$  are the pathogen concentrations for the influent and effluent, respectively.

Different countries have established regulatory requirements to undertake challenge testing to validate membrane performance for virus removal. The United States Environmental Protection Agency (U.S. EPA) has promulgated the Long Term 2 Enhanced Surface Water Treatment Rule and Stage 2 Disinfectants and Disinfection By-product Rule, which include detailed requirements for membrane challenge testing [25]. In Australia, the Victorian Department of Health and Human Services has issued Guidelines for Validating Treatment Processes for Pathogen Reduction in 2013 [26]. It requires that an annual challenge test to be undertaken using either seeded MS2 bacteriophage or indigenous FRNA bacteriophage to confirm the extent of virus removal by membrane processes. If a membrane system fails to meet the previously credited LRV in the challenge test, remedial action has to be undertaken. Water supply can only resume after compliance of the credited LRV is validated.

Australian Guidelines for Water Recycling: Managing Health and Environmental Risks [27] has established different health-based performance targets for the microbial quality of recycled water sourced from wastewater (Table 2).

In this study, a water utility experienced multiple validation failures in one of its UF plants with virus log reduction values (LRV) as low as 0.79 reported. This resulted in the suspension of recycled water supply to customers and initiated a comprehensive root cause analysis to identify the reason for the unusually rapid membrane degradation and virus removal validation failure. As a result of the root cause analysis, several system improvements were implemented including system control, new inline static mixer, CEB water quality monitoring, etc. The remediation procedures have been successful in maintaining the maximum virus LRV of 4 for the UF system.

This root cause analysis highlights the critical role of operation in maintaining the effective virus removal of membrane system. It also provides key insight into the different technologies used for membrane integrity monitoring. When UF is used as the pre-treatment for RO process in a desalination plant or as a standalone process for virus removal, the steps outlined in this study could facilitate the identification of key operational issues or opportunities for improvement and optimisation of membrane plants.

# 2. Materials and methods

# 2.1. Study site

#### 2.1.1. Recycled water treatment plant (RWTP)

The studied RWTP is located in the south eastern region of Melbourne, Australia. The plant was commissioned in 2009 with a mean daily flowrate of  $12,000~\text{m}^3/\text{d}$ . The UF process comprises part of the treatment train for production of recycled water as shown in Fig. 1. Wastewater is first processed through an activated sludge-based treatment plant and the resulting secondary effluent is further pre-treated by straining. To improve virus removal by UF membrane, coagulant (aluminium chlorohydrate (ACH)) can also be dosed into the influent to

**Table 2**Targeted LRVs for different uses of recycled water sourced from wastewater.

Use of recycled water	LRVs		
	Protozoa	Virus	Bacteria
Commercial food crops	4.8	6.1	5.0
Garden irrigation	4.4	5.8	4.6
Municipal irrigation	3.7	5.2	4.0
Fire fighting	5.1	6.5	5.3

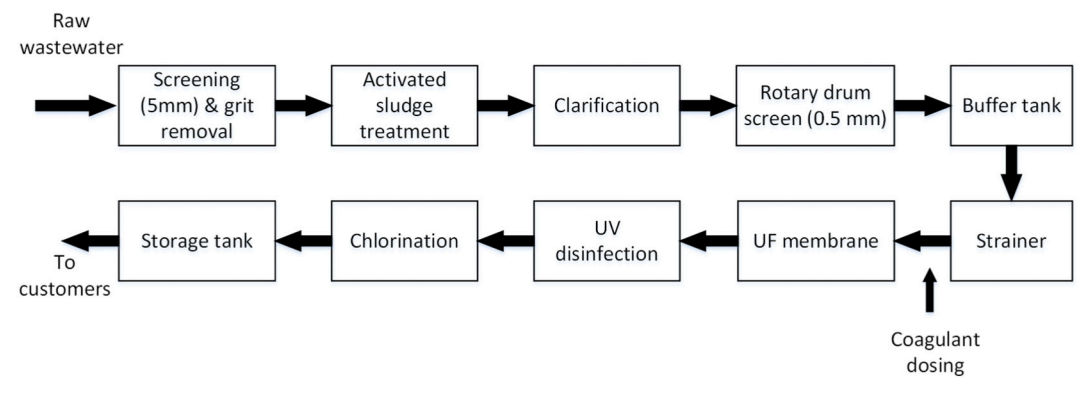


Fig. 1. Process flow diagram for the RWTP.

the UF membrane. Following coagulation, the effluent is filtered through the UF train prior to UV disinfection and chlorination prior to storage. The final effluent is predominantly used for farm irrigation of fruits, vegetables and flowers.

Based on the Victorian Guidelines for Validating Treatment Processes for Pathogen Reduction [26], the maximum virus LRV credited to a single treatment process is 4. The highest virus LRV credits for activated sludge process, UF process, and chlorination are 0.5, 4, and 4, respectively.

Australian Guidelines for Water Recycling: Managing Health and Environmental Risks [27] establishes the virus LRV requirement of 6.1, when the recycled water is used for commercial food crop irrigation. As the effluent from the studied RWTP is used for farm irrigation of fruits, vegetables and flowers, the minimum threshold virus LRV for UF process is 1.6, if activated sludge process and chlorination are operated within their optimal conditions and their maximum LRVs are maintained.

#### 2.1.2. Membrane properties

The UF plant was built and commissioned in 2009, and the system was validated to have 4 LRV for virus. Detailed characteristics of the UF process are shown in Table 3.

# 2.2. Membrane autopsy methods

#### 2.2.1. Sampling

Two poor performing membrane modules were removed from service and a new membrane module was provided as a control. The membranes were cut open with an oscillating cast saw, visually inspected and photographed. The membrane module configuration is such that there are 12 segments containing individual fibres separated by spacers around a central permeate collection tube. For the new membrane, 1 fibre bundle was collected for analysis and benchmark testing. For the used membranes, 3 fibre bundles from non-adjacent segments were collected for testing. The fibres from the modules were designated as top, middle and bottom with reference to the capping (top) and samples were taken from different locations as shown in Fig. 2.

**Table 3** Characteristics of the UF process.

Process design	Description	
Skids	4	
Vessels per skid	24	
Modules per vessel	4	
Membrane area per skid	3840 m <sup>2</sup>	
Membrane material	PES/PVP blend <sup>a</sup>	
Nominal pore size	20 nm	
Designed flux	59 L/m <sup>2</sup> .h	
Flow mode	Dead-end	
Flow configuration	Inside-out	

<sup>&</sup>lt;sup>a</sup> PES: polyethersulfone, PVP: polyvinylpyrrolidone.

Membrane fibres were subjected to structural analysis (Fourier-transform infrared (FTIR) spectroscopy), thermal analysis (differential scanning calorimetry, DSC), surface charge (streaming potential, SP), high resolution imaging with elemental analysis (scanning electron microscopy, SEM with energy dispersive spectroscopy, EDS), tensile testing, and qualitative pore size (QPS) evaluation. Samples for FTIR and SEM/EDS were further prepared by cutting sample fibres open to enable analysis of the inner skin layer. For some of the analyses, fibre samples were rinsed and dried overnight in an air-circulating oven at 40 °C. The new membrane fibres were packed with a preservative which was washed from the surfaces prior to testing.

#### 2.2.2. Structural analysis

FTIR spectroscopic analysis was used to determine the possible changes in the membrane chemical structures of the membrane surfaces. A Perkin Elmer Frontier FTIR spectrophotometer (Perkin Elmer, Waltham, USA) with a diamond crystal attenuated total reflectance (ATR) attachment was used to scan the surface of the membranes. Cleaned and dried membrane samples were clamped onto the ATR crystal and the wavelength range  $4000{-}700~\rm{cm}^{-1}$  was scanned with a minimum of 8 scans accumulated per sample. Both the inner and outer surfaces were scanned with the inner surfaces exposed by cutting the fibres with a scalpel blade and samples from each location were averaged.

# 2.2.3. Thermal analysis

Differential scanning calorimetry was used to assess macromolecular changes in the PES polymer by measuring the glass transition temperature ( $T_g$ ). A Mettler Toledo DSC1 instrument (Mettler Toledo, Greifensee, Switzerland) was used with samples of the PES scraped from the inner surfaces of the membrane samples with a scalpel blade. Samples of approx. 10 mg were sealed in aluminium crucibles and were heated over the temperature range 50–250 °C at a rate of 10 °C/min under a nitrogen atmosphere. Sample results from fibres in each set were averaged.

# 2.2.4. Streaming potential analysis

Streaming potential analysis was performed to determine the surface charge of the fibres using an Anton Paar SurPASS2 electrokinetic analyzer (Anton Paar, Graz, Austria). Fibres of 5 cm lengths were inserted into an adapter to enable the measurement of the inner surface using the cylindrical cell settings. The streaming potential measurements were performed over the pH range ca. 9–3 in 0.001 M KCl solution and the results are the average of 4 measurements at each pH. Sample results of the fibres from each set were averaged.

#### 2.2.5. Surface and cross-section imaging

Fibre imaging of the surfaces from the middle section of fibre samples were performed using a ZEISS Merlin Gemini 2 Field Emission SEM (Zeiss International, Oberkochen, Germany) in high-resolution column mode with images recorded at 3 kV and at magnifications of up to

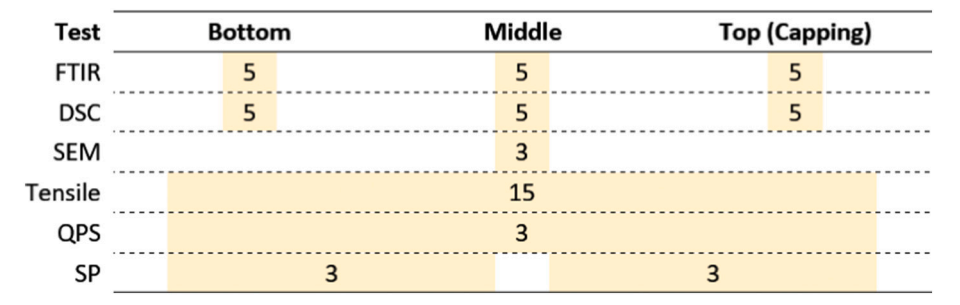


Fig. 2. Fibre sampling locations (shaded) and minimum number of samples tested.

 $1000\times.$  Prior to imaging, all samples were sputter-coated with iridium using a Polaron SC5750 sputter coater (Quorum Technologies, Laughton, UK). To observe the inner surfaces, samples were cut using ultrasharp blades.

#### 2.2.6. Tensile testing

Tensile tests were performed using a Model 4301 Instron Universal Testing Machine (Instron, Norwood, MA, USA) with a load cell of 5 kN using a cross-head speed of 10 mm  $\rm min^{-1}$ . A minimum of 15 fibre samples of 100 mm length from each of the new and used membrane were tested. The average load at break (tensile strength) and percentage extension at break were measured using Instron BlueHill Series IX software (Instron, Norwood, MA, USA). The average and standard deviation between the samples was determined.

#### 2.2.7. Qualitative pore size evaluation

A series of challenge tests were performed to evaluate the apparent porosity of the membrane fibres utilizing four sets of fluorescent nanoparticles (NPs) of average sizes 50, 110, 150 and 185 nm with a narrow size distribution. A series of up to 9 fibres of 40 cm length were potted in epoxy and connected to a peristaltic pump attached to a feed vessel containing the nanoparticles (up to 10 mg/L). The challenge tests were performed by pumping the feedwater through the membranes, collecting and testing the permeate for the presence of the particles by fluorescence detection using a Horiba Aqualog fluorescence spectrofluorometer (Horiba, Kyoto, Japan). Between tests, the membranes were back-flushed with MilliQ water to remove any particles from inside of the fibres.

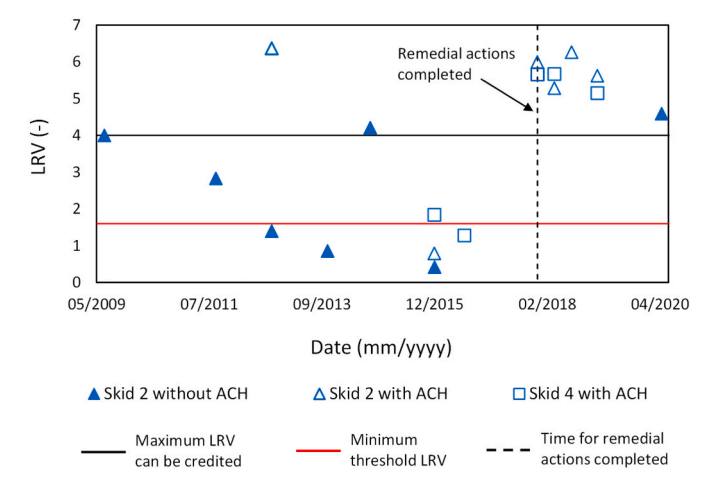


Fig. 3. UF membrane multiple validation failures for virus LRV credit.

# 3. Results and discussion

#### 3.1. Membrane system validation failures in virus removal

Fig. 3 shows the history of UF membrane challenge test results between 2011 and 2016. The black line indicates that the maximum virus LRV of 4 can be credited to UF process, although challenge tests could show higher LRV. The red line indicates the minimum threshold virus LRV of 1.6, which is the minimum virus removal requirement for the UF process to ensure the RWTP is able to meet the required LRV of 6.1 for the total process. The black dot line indicates the time when the remedial actions have been completed. Only the results for skids with the worst virus removal performance are shown in Fig. 3.

It is clearly shown that the UF membrane could effectively remove virus when the plant was commissioned in 2009. In September 2011, the virus LRV reduced to 2.83, it was still higher than the threshold virus LRV of 1.6. In October 2012, the online membrane integrity monitoring (diffusive air-flow test) did not detect membrane integrity issue. However, the MS2 challenge test identified that the virus LRV further reduced to 1.4, and the minimum virus LRV of 1.6 could not be met.

The operations team commenced dosing ACH to improve virus removal, and the challenge test results showed that the LRV of 6.37 could be obtained with ACH dosing, so skid 2 was then operated with ACH dosing. It was identified that the virus LRV further reduced to 0.86 for skid 2 in November 2013 if ACH was not used. The UF membrane was subsequently replaced after only 4 years operation.

The challenge test in September 2014 showed that the virus LRV could be maintained above 4 for 1 year following membrane replacement. However, a challenge test in December 2015 showed that the virus LRVs for skids 2 and 4 were only 0.79 and 1.84, respectively, even with ACH dosing. Skid 2 was then taken offline. Skid 4 could still be used since the minimum virus LRV of 1.6 was met. In July 2016, another challenge test was organised for skid 4 and the results showed that virus LRV of 1.28 could only be achieved.

The rapid decline in membrane virus LRV was highly unusual, and the entire UF membrane process was taken offline and a comprehensive investigation was performed to identify the root cause for the observed change in LRV. New membranes were installed in December 2017 after remedial actions were implemented and the virus LRV has been maintained above 4 since then. Although the challenge test result from May 2020 showed a slightly decline of the virus LRV, it was still higher than 4 and no ACH was used during the MS2 challenge test.

#### 3.2. Membrane autopsy evaluation results

#### 3.2.1. Visual inspection

Fig. 4 shows photographs of one used element in various stages of the autopsy, which was representative of the condition of both used elements. The ends of the element showed evidence of pinning and discoloration (Fig. 4(a)). In addition, there was evidence of rust deposits on the outer PVC shell on one end of the element (Fig. 4(b)). A section of the PVC casing was removed to reveal the membrane fibres (Fig. 4(c))

# (a) Membrane end



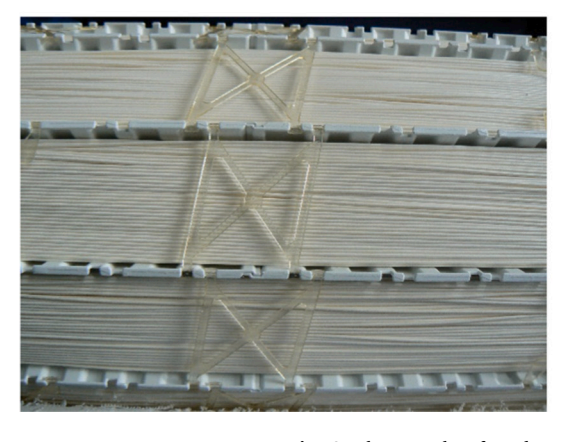
# (b) Outer casing



(c) Whole membrane element, casing removed



# (d) Used fibres secured in channels



# (e) Used fibres extracted for testing



Fig. 4. Photographs of used membrane element during autopsy.

which were intact and secured in the various channels (Fig. 4(d)). The outer surfaces of the membrane fibres showed the evidence of discolouration although no visible foulants or deposits were observed (Fig. 4(e)). There was no evidence of blocked pores on either end of the element and no evidence of broken fibres. The new element was similar in appearance but was not discoloured (photographs not shown).

#### 3.2.2. FTIR analysis

The membrane fibres were constructed of PES (diphenylenesulfone

and aromatic ether repeating units [28]) and PVP (amide and C=O functional groups [29]) and these polymers are readily identifiable by FTIR spectroscopy. The FTIR spectrum of the inner surface of the new membrane sample is shown in Fig. 5 highlighting the characteristic peaks of PES (sulfur, ester and aromatic groups) and PVP (amide and carbonyl groups) [29–34]. There is a peak at 1743 cm<sup>-1</sup> on the outer surface and a peak at 1671 cm<sup>-1</sup> on the inner surface which are both absent on the opposite sides (see inset in Fig. 5). These peaks are consistent with PVP suggesting different levels of this polymer are

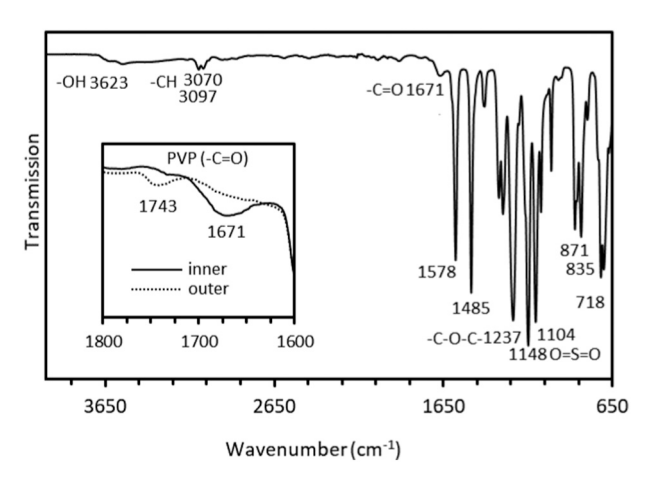


Fig. 5. FTIR spectra of new membrane inner surface.

present on the outer and inner surfaces.

Fig. 6 shows the spectra of the new and used membrane inner surfaces in selected regions highlighting some key differences between the membrane samples. The intensities of the broad -OH peaks are higher in the used membrane spectrum, which is not uncommon in aged membranes (Fig. 6(a)). The peaks that are characteristic of PVP (Fig. 6(b)) have changed in intensity and wavenumber which suggests changes in the PVP concentration and/or composition on the surface [31,33]. There is a new peak at 1031 cm<sup>-1</sup> on the used membrane sample (Fig. 6(c)), which suggested the presence of sulfonic acid due to chlorine oxidation of the membrane surface [33].

Fig. 7(a) shows the spectra of the new and used membrane fibres (outer surface) in the region 4000–2600 cm<sup>-1</sup> with some distinct differences between samples. There are new peaks in the used sample at 3700 and 3620 cm<sup>-1</sup> that are associated with —OH vibrations. The —CH peaks have reduced in intensity which may suggest a loss of PVP on the outer surface, however, a loss of PVP from membranes is not uncommon and does not necessarily result in integrity issues. Changes in composition are also observed in the region 1150–650 cm<sup>-1</sup> (Fig. 7(b)) including a new peak on the used membrane spectrum at 1034 cm<sup>-1</sup> which may be due to the presence of sulfonic acid [33] and/or the presence of an orthophenol substitution on the PES structure [29]. A new peak is also present at 913 cm<sup>-1</sup> on the used membrane surface which may be due carboxylic acid as a result of chlorine oxidation of the PES. It has been shown that PES membranes can rapidly oxidize when exposed to hypochlorite [35].

## 3.2.3. Thermal properties

Polyethersulfone is a relatively linear polymer with aromatic groups

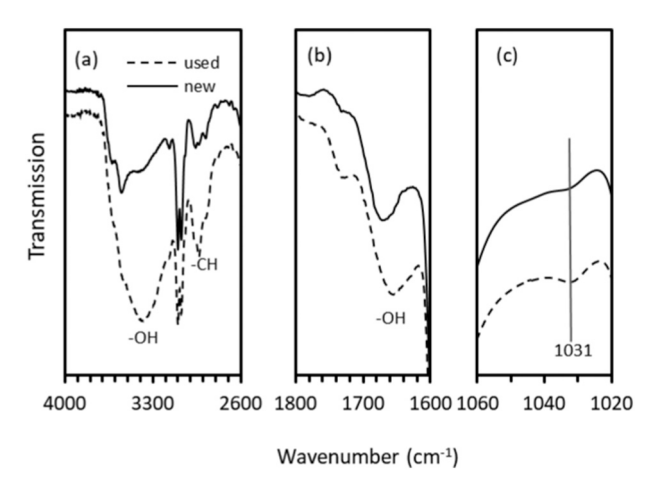


Fig. 6. Inner surface FTIR spectra of new and used membranes.

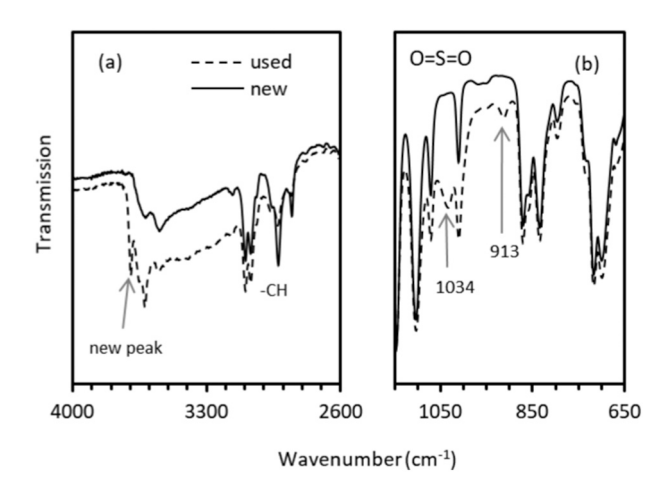


Fig. 7. Outer surface FTIR spectra of new and used membranes.

spaced between SO<sub>2</sub> groups and ether linkages. The polymer is unable to readily form crystals and is, therefore, primarily amorphous in structure [28] with a high glass transition temperature ( $T_g > 230\,^{\circ}$ C) [28,29]. Similarly, PVP is an amorphous polymer with a high  $T_g$  (180–190 °C) [36]. As shown in Table 4, thermal analysis of the new membrane samples using DSC showed two phase transitions consistent with PVP and PES respectively. The used membrane samples showed only a single  $T_g$  consistent with PES and no evidence of a  $T_g$  for PVP. The PES  $T_g$  values and associated  $\Delta$ H values were lower for the used membranes suggesting some changes in the PES. This is consistent with the FTIR analyses (Fig. 6) and may be due to changes in the O=S=O bonds and/or the loss of PVP. Changes in the PES structures may alter the conformation of the bond linkages facilitating bending and reducing stiffness.

#### 3.2.4. Streaming potential (SP)

The SP as a function of pH for the new and used membrane fibres is shown in Fig. 8. The surface charges of both new and used membranes increased from high to low pH with a significant difference between the negativity of the surfaces. The used membrane samples were less negative over the entire pH range and this was more significant over the alkaline pH range. The SP of membranes generally increases when surfaces are fouled [37] and chemical changes in polymer structures such as oxidation can also influence surface charge [38].

#### 3.2.5. Fibre imaging

Imaging was performed on surfaces of the membrane fibre samples using SEM/EDS as shown in Fig. 9. Imaging and EDS analysis of the new membrane (Fig. 9(a)) showed only C, O, and S which are present in PES and this was also observed for the inner surface (data not shown). The used membrane outer surface (Fig. 9(b)) shows some evidence of particulates which were comprised of Si, Al, Fe, Cl, and other trace elements that are consistent with silicate fouling. This is also consistent with the presence of the new peak observed in the FTIR spectra which may be due to silicates [39].

Fig. 9(c) shows the inner surface of the used membrane samples with evidence of more extensive particulate fouling. In this case, the EDS analysis showed the selected particulates were comprised of Cl, K, Na, Al, with some trace Ca and Si suggesting the presence of salts and trace

**Table 4**DSC analysis of new and used membrane fibres.

Sample	Component	<i>T</i> <sub>g</sub> (°C)	$\Delta H (J g^{-1})$
New	PVP	$191.9 \pm 5.8$	$41.97 \pm 2.02$
	PES	$231.1\pm0.2$	$0.98 \pm 0.05$
Used	PVP	Not detected	Not detected
	PES	$228.1\pm1.4$	$0.77\pm0.12$

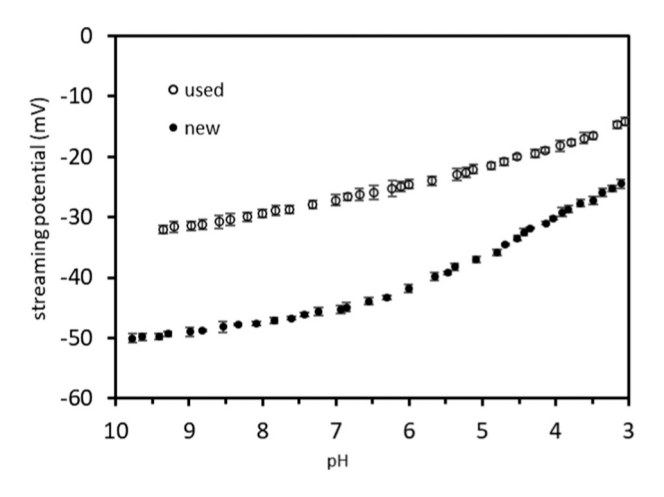


Fig. 8. Streaming potential of membrane fibre surfaces.

silicates.

#### 3.2.6. Tensile properties

Tensile testing was performed to evaluate physicomechanical changes in the membrane fibres and the results are shown in Fig. 10. The force required to break the used fibre is ca. 9% lower than the new fibre suggesting some changes in the PES material. The elongation at break of the used fibre was ca. 47% lower than the new fibre suggesting significantly reduced elasticity. These results are consistent with ageing of the membrane material and may contribute to the reduced LRV observed.

#### 3.2.7. Qualitative porosity

The apparent porosity of the membranes was qualitatively measured by subjecting the fibres to fluorescent nanoparticle challenge tests (Table 5). The new membrane fibres were able to reject all the challenge particles and this is consistent with the nominal pore size of 20 nm for this membrane element. In contrast, the used membranes failed to reject most challenge particles suggesting that there are a significant number of pores that are greater than ca. 20 nm, which could allow virus to be passed. This confirms the previously determined MS2 challenge test results with low LRVs.

# 3.3. Root cause analysis and remedial actions

The used membranes were visually similar in appearance to the new membranes with no visible deposits observed on the outer surface (permeate side). However, some discoloration (yellowing) of the outer surfaces of the used fibres was observed. Both the inner and outer surfaces showed some differences in the FTIR spectra suggesting some changes in the PES and PVP structures. The changes included some new unidentified peaks on the outer surface of the used fibres and overall, the results indicated the high possibility of oxidative damage of the fibres.

The DSC analyses showed changes in the  $T_{\rm g}$  of PES and the absence of a  $T_{\rm g}$  for PVP in the used membrane which suggested changes in the polymer structures and morphology. The lower  $T_{\rm g}$  of PES and the chemical changes observed in the FTIR results also suggested changes in the polymer backbone resulting in greater flexibility of the polymer chains. Increased surface charge of the used fibres was observed which was probably due to the oxidative damage and/or surface fouling. The SEM/EDS analysis of particles on inner and outer surfaces revealed the presence of silicate compounds (Al, trace Fe) and salts, and this was probably introduced by the backwash and/or chemical enhanced backwash (CEB) processes. The tensile results showed a decline in the mechanical integrity of the fibres and challenge testing revealed a loss of integrity allowing the passage nanoparticles larger than the MS2 bacteriophage.

The above results suggested that the unusually rapid membrane degradation was probably due to chemical oxidation of the PES fibres. A detailed on-site investigation was then undertaken and it was identified that the failure to operate the appropriate CEB was the main cause for the unusually rapid virus LRV reduction.

There are two CEB cycles for the membrane installation and stored membrane permeate is used for backwashing. Hypochlorite is added into the permeate prior to its storage. For the first CEB cycle, combined sodium hydroxide and sodium hypochlorite are dosed into the backwash line to chemically clean the membrane. For the second CEB cycle, combined sulphuric acid and sodium metabisulphite (SMBS) are dosed to neutralize the free chlorine present in the permeate backwash water and execute an acid backwash.

A static mixer is usually installed in the backwash inlet line downstream of the chemical dosing points, which ensures the sufficient mixing of different chemicals during the CEB. Site investigation identified that the inline static mixer was not installed. This could lead to highly concentrated chemicals entering the membranes subsequently causing the damage observed. It was also identified that there were no backpressure or anti-siphoning valve installed in the CEB chemical dosing lines, which could result in chemical dosing at a higher rate than the designated pumping rate due to the siphoning effect.

Further investigations identified that the amount of CEB chemicals were calculated based on the backwash flowrate, and there was no monitoring or feedback to control the chemical dosing amounts. For the first CEB cycle, if sodium hydroxide is not dosed proportionally to sodium hypochlorite, this may lead to a lower pH and subsequently membrane chemical oxidation. For the second CEB cycle, if SMBS is not adequately dosed to neutralize the free chlorine, this could also contribute to the oxidation observed on the membrane surface. It was recommended that flow meters should be installed on all chemical dosing lines with output connected to the supervisory control and data acquisition (SCADA) system. The measured values should be automatically compared to pre-set values with alarms indicating any deviation. Furthermore, no pH or oxidation-reduction potential (ORP) meter was installed in the backwash inlet line and therefore high or low pH/ORP values cannot be alarmed, which could lead to excessive oxidation of the membranes.

The actual CEB water sampling and analysis were performed, which confirmed that free chlorine was considerably higher than the manufacturer's suggested chlorine concentration for both first and second CEB cycles.

Supported by the membrane autopsy study, desktop/site investigation, and actual CEB water sampling and analysis, system improvements (system control, new inline static mixer, CEB water quality monitoring, etc.) were implemented in December 2017 based on the root cause analysis, and the virus LRV has been maintained above 4 since then.

# 4. Conclusions

A UF membrane integrity issue was encountered at a water utility which resulted in the suspension of recycled water supply to customers. Multiple validation failures in annual MS2 challenge tests were not identified using the more frequent online diffusive air-flow test. To investigate the virus removal validation failure, a comprehensive root cause analysis was performed in order to remediate the issue and restore the plant to capacity.

A membrane autopsy was performed and involved removal and sampling of poor performing elements. Following visual inspection, membrane fibres were sampled from the modules and the autopsy analyses identified changes in the membrane chemistry, morphology, and mechanical strength. In addition, the membranes were unable to reject the fluorescent nanoparticles that were smaller than 150 nm. The overall results suggested that the observed rapid membrane degradation was probably due to the chemical oxidation.

A detailed on-site investigation at the plant identified that an inline

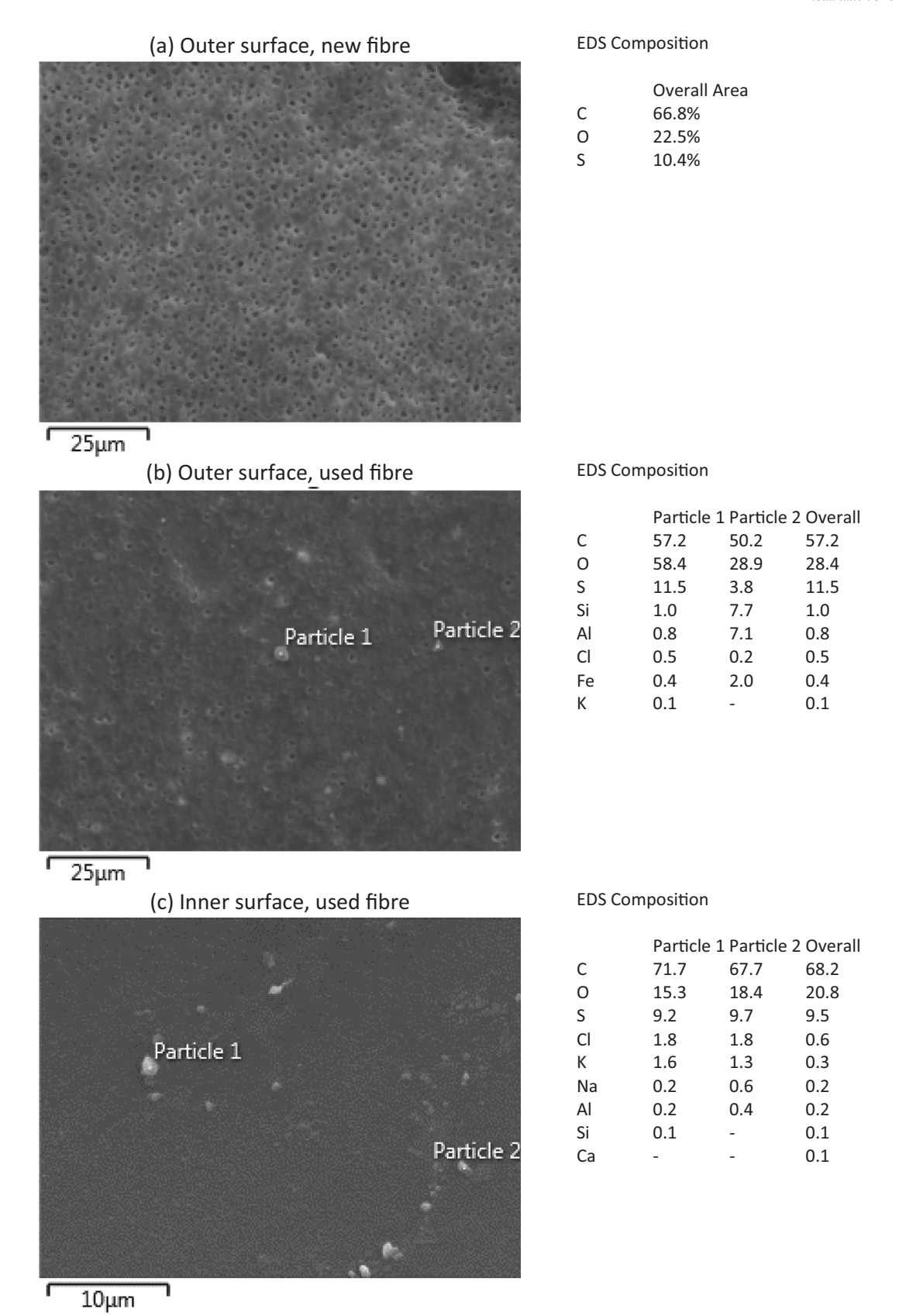


Fig. 9. SEM images of membrane surfaces.

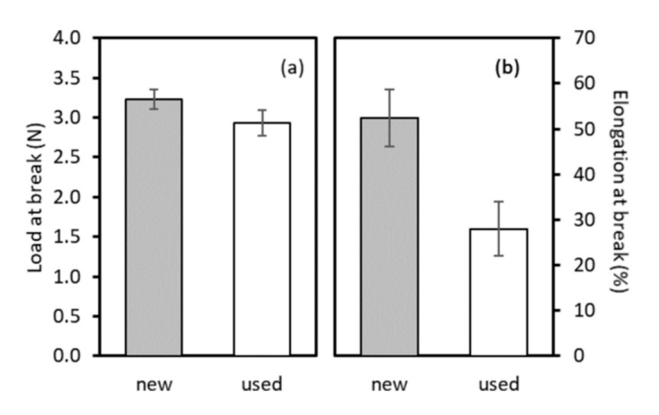


Fig. 10. Tensile load at break (a) and elongation at break (b) of new and used membrane fibres.

**Table 5**Particle challenge test rejection results.

	Challenge particle size range <sup>a</sup> (nm)				
Membrane	40–60 (55)	75–125 (110)	120–170 (150)	140-200 (185)	
New Used	Rejected No rejection	Rejected No rejection	Rejected No rejection	Rejected Partial rejection	

<sup>&</sup>lt;sup>a</sup> Peak nanoparticle size given in brackets.

static mixer was not installed in the backwash inlet line downstream of the chemical dosing points. In addition, there were no backpressure or anti-siphoning valves installed in the CEB chemical dosing lines and there was no control or feedback to control the chemical dosing amounts. These issues may have contributed to the higher chemical dosing resulting in the oxidation observed on the membrane surface and the subsequent decline in membrane integrity. Sampling and analysis of the CEB water were performed and confirmed that free chlorine was considerably higher than the manufacturer's suggested chlorine concentration for the CEB cycles.

As a result of the root cause analysis, several system improvements were implemented including system control, new inline static mixer, CEB water quality monitoring, etc. The remediation procedures have been successful in maintaining the maximum virus LRV of 4 for the UF system.

# CRediT authorship contribution statement

**Marlene Cran:** Methodology, Formal analysis, Investigation, Writing - Original Draft, Writing - Review & Editing.

 $\begin{tabular}{ll} \textbf{Stephen Gray:} Formal analysis, Investigation, Supervision, Writing - Review \& Editing. \end{tabular}$ 

 $\textbf{Jonathan Schmidt:} \ \ Conceptualization, \ Formal \ analysis, \ Investigation, \ Writing \ - \ Review \ \& \ Editing.$ 

**Li Gao:** Writing - Original Draft, Writing - Review & Editing, Formal analysis, Funding acquisition.

## Declaration of competing interest

The authors declare that they have no known competing financial interests or personal relationships that could have appeared to influence the work reported in this paper.

# Acknowledgements

The authors gratefully acknowledge the funding, data contribution and support from South East Water. The authors also acknowledge the technical support from Aqueous Solutions (Victoria, Australia).

#### References

- L. Gao, J. Zhang, G. Liu, Life cycle assessment for algae-based desalination system, Desalination 512 (2021), 115148.
- [2] G.-Q. Li, W.-L. Wang, Z.-Y. Huo, Y. Lu, H.-Y. Hu, Comparison of UV-LED and low pressure UV for water disinfection: photoreactivation and dark repair of Escherichia coli, Water Res. 126 (2017) 134–143.
- [3] T.S. Natarajan, M. Thomas, K. Natarajan, H.C. Bajaj, R.J. Tayade, Study on UV-LED/TiO2 process for degradation of rhodamine B dye, Chem. Eng. J. 169 (2011) 126–134.
- [4] W. Feng, Y. Liu, L. Gao, Stormwater treatment for reuse: current practice and future development – a review, J. Environ. Manag. 301 (2022), 113830.
- [5] J. Sun, B. Li, Q. Wang, P. Zhang, Y. Zhang, L. Gao, X. Li, Preparation of phosphorus-doped tungsten trioxide nanomaterials and their photocatalytic performances, Environ. Technol. (2020) 1–11.
- [6] J. Wei, L. Gao, G. Shen, X. Yang, M. Li, The role of adsorption in microalgae biological desalination: salt removal from brackish water using Scenedesmus obliquus, Desalination 493 (2020) 114616.
- [7] M. Kube, B. Spedding, L. Gao, L. Fan, F. Roddick, Nutrient removal by alginateimmobilized Chlorella vulgaris: response to different wastewater matrices, J. Chem. Technol. Biotechnol. 95 (2020) 1790–1799.
- [8] L. Gao, X. Zhang, L. Fan, S. Gray, M. Li, Algae-based approach for desalination: an emerging energy-passive and environmentally friendly desalination technology, ACS Sustain. Chem. Eng. 9 (2021) 8663–8678.
- [9] L. Gao, J. Zhang, S. Gray, J.-D. Li, Modelling mass and heat transfers of permeate gap membrane distillation using hollow fibre membrane, Desalination 467 (2019) 196–209
- [10] L. Gao, J. Zhang, S. Gray, J.-D. Li, Influence of PGMD module design on the water productivity and energy efficiency in desalination, Desalination 452 (2019) 29–39.
- [11] R. Singh, R. Bhadouria, P. Singh, A. Kumar, S. Pandey, V.K. Singh, Nanofiltration technology for removal of pathogens present in drinking water, Waterborne Pathogens (2020) 463–489.
- [12] A.M. ElHadidy, S. Peldszus, M.I. Van Dyke, An evaluation of virus removal mechanisms by ultrafiltration membranes using MS2 and φX174 bacteriophage, Sep. Purif. Technol. 120 (2013) 215–223.
- [13] Alternative disinfectants and oxidants guidance manual, US Environmental Protection Agency, Office of Water, United States, 1999.
- [14] G. Herath, K. Yamamoto, T. Urase, Removal of viruses by microfiltration membranes at different solution environments, Water Sci. Technol. 40 (1999) 331–338.
- [15] S.S. Madaeni, A. Khorasani, M. Asgharpour, S.A. Ghoreshi, M. Lotfi, Removal of mixtures of viruses using microfiltration membrane, Desalin. Water Treat. 51 (2013) 4313–4322.
- [16] G. Carvajal, A. Branch, S.A. Sisson, D.J. Roser, B. van den Akker, P. Monis, P. Reeve, A. Keegan, R. Regel, S.J. Khan, Virus removal by ultrafiltration: understanding long-term performance change by application of bayesian analysis, Water Res. 122 (2017) 269–279.
- [17] P. Reeve, R. Regel, J. Dreyfus, P. Monis, M. Lau, B. King, B. van den Akker, Virus removal of new and aged UF membranes at full-scale in a wastewater reclamation plant 2 (2016) 1014–1021.
- [18] Pore Size, Pore size distribution, and roughness at the membrane surface, in: K. C. Khulbe, C.Y. Feng, T. Matsuura (Eds.), Synthetic Polymeric Membranes: Characterization by Atomic Force Microscopy, Springer, Berlin Heidelberg, Berlin, Heidelberg, 2008, pp. 101–139.
- [19] A. Antony, J. Blackbeard, G. Leslie, Removal efficiency and integrity monitoring techniques for virus removal by membrane processes, Crit. Rev. Environ. Sci. Technol. 42 (2012) 891–933.
- [20] M. Li, L. Gao, L. Lin, Specific growth rate, colonial morphology and extracellular polysaccharides (EPS) content of Scenedesmus obliquus grown under different levels of light limitation, Ann. Limnol. Int. J. Limnol. (2015) 329–334. EDP Sciences.
- [21] M. Li, W. Zhu, L. Gao, J. Huang, L. Li, Seasonal variations of morphospecies composition and colony size of microcystis in a shallow hypertrophic lake (Lake Taihu, China), J. Fresen. Environ. Bull. 22 (2013) 3474–3483.
- [22] P.H. Wolf, S. Siverns, S. Monti, UF membranes for RO desalination pretreatment, Desalination 182 (2005) 293–300.
- [23] P.-Y. Hong, N. Moosa, J. Mink, Dynamics of microbial communities in an integrated ultrafiltration–reverse osmosis desalination pilot plant located at the Arabian Gulf, Desalin. Water Treat. 57 (2016) 16310–16323.
- [24] C. Schang, J. Schmidt, L. Gao, D. Bergmann, T. McCormack, R. Henry, D. McCarthy, Rainwater for residential hot water supply: managing microbial risks, Sci. Total Environ. 782 (2021), 146889.
- [25] N.K. Shammas, L.K. Wang, Membrane filtration regulations and determination of log removal value, in: L.K. Wang, J.P. Chen, Y.-T. Hung, N.K. Shammas (Eds.), Membrane and Desalination Technologies, Humana Press, Totowa, NJ, 2011, pp. 135, 190
- [26] S. Sarkis, L. Richard, V. Mulvenna, R. Poon, D. Deere, in: Guidelines for validating treatment processes for pathogen reduction, Department of Health, State of Victoria, Melbourne, 2013, pp. 1–80.
- [27] Australian guidelines for water recycling: managing health and environmental risks (Phase 1), in, Canberra, Australia, 2006.
- [28] S. Ida, PES (poly(ether sulfone)), polysulfone, in: Encyclopedia of Polymeric Materials, Springer-Verlag, Berlin, Heidelberg, 2014, pp. 1–8.
- [29] B. Pellegrin, R. Prulho, A. Rivaton, S. Thérias, J.-L. Gardette, E. Gaudichet-Maurin, C. Causserand, Multi-scale analysis of hypochlorite induced PES/PVP ultrafiltration membranes degradation, J. Membr. Sci. 447 (2013) 287–296.

- [30] K. Boussu, J. De Baerdemaeker, C. Dauwe, M. Weber, K.G. Lynn, D. Depla, S. Aldea, I.F.J. Vankelecom, C. Vandecasteele, B. Van der Bruggen, Physico-chemical characterization of nanofiltration membranes, ChemPhysChem 8 (2007) 370–379.
- [31] H. Wang, T. Yu, C. Zhao, Q. Du, Improvement of hydrophilicity and blood compatibility on polyethersulfone membrane by adding polyvinylpyrrolidone, Fibers Polym. 10 (2009) 1–5.
- [32] L. Saravanan, S. Diwakar, R. Mohankumar, A. Pandurangan, R. Jayavel, Synthesis, structural and optical properties of PVP encapsulated CdS nanoparticles, Nanomater. Nanotechnol. 1 (2011) 42–48.
- [33] R. Prulho, S. Therias, A. Rivaton, J.-L. Gardette, Ageing of polyethersulfone/ polyvinylpyrrolidone blends in contact with bleach water, Polym. Degrad. Stabil. 98 (2013) 1164–1172.
- [34] S. Salgin, U. Salgin, N. Soyer, Streaming potential measurements of polyethersulfone ultrafiltration membranes to determine salt effects on membrane zeta potential, Int. J. Electrochem. Sci. 8 (2013) 4073–4084.
- [35] C. Causserand, S. Rouaix, J.-P. Lafaille, P. Aimar, Ageing of polysulfone membranes in contact with bleach solution: role of radical oxidation and of some dissolved metal ions, Chem. Eng. Process. 47 (2008) 48–56.
- [36] K. Lewandowska, The miscibility of poly(vinyl alcohol)/poly(N-vinylpyrrolidone) blends investigated in dilute solutions and solids, Eur. Polym. J. 41 (2005) 55–64.
- [37] N.D. Lawrence, J.M. Perera, M. Iyer, M.W. Hickey, G.W. Stevens, The use of streaming potential measurements to study the fouling and cleaning of ultrafiltration membranes, Sep. Purif. Technol. 48 (2006) 106–112.
- [38] M. Pontié, Effect of aging on UF membranes by a streaming potential (SP) method, J. Membr. Sci. 154 (1999) 213–220.
- [39] S.J. Parikh, K.W. Goyne, A.J. Margenot, F.N.D. Mukome, F.J. Calderón, Soil chemical insights provided through vibrational spectroscopy, in: L.S. Donald (Ed.), Advances in Agronomy, Academic Press, 2014, pp. 1–148.